An evaporitic origin of the parent brines of Colombian emeralds: fluid inclusion and sulphur isotope evidence

GASTON GIULIANI[1,2]*, ALAIN CHEILLETZ[2,3], CARLOS ARBOLEDA[4],
VICTOR CARRILLO[4], FÉLIX RUEDA[4] and JAMES H. BAKER[5]

[1] ORSTOM, Institut Français de Recherche Scientifique pour le Développement en Coopération,
213 rue La Fayette, 75480 Paris cedex 10, France

[2] CRPG-CNRS, Centre de Recherches Pétrographiques et Géochimiques, BP 20,
54501 Vandoeuvre-lès-Nancy cedex, France

[3] ENSG-INPL, Ecole Nationale Supérieure de Géologie, BP 452,
54001 Nancy cedex, France

[4] MINERALCO S.A, calle 32, N°13-07, Apartado 17878, Bogotá, Colombia

[5] State University of Utrecht, Institute for Earth Sciences, PO Box 80.021,
3508 TA Utrecht, The Netherlands

Abstract: The fluids trapped by emerald, dolomite and pyrite in the Colombian emerald deposits consist predominantly of Na-Ca brines with some KCl. The similarity of fluid composition in the eastern and western emerald zones demonstrates the homogeneity of the parent fluids. The Na-Ca-K chemistry of the brines provides strong evidence for an evaporitic origin of the parent hydrothermal fluids. Their origin was investigated by a sulphur isotopic study of pyrite that coprecipitated with emerald. The $\delta^{34}S$ values of H_2S in solution in equilibrium with pyrite from six emerald deposits range from 14.8 to 19.4 ‰ whereas sedimentary pyrite from the enclosing black shales yield a $\delta^{34}S$ of -2.4 ‰. The narrow range in $\delta^{34}S_{H2S}$ between the different deposits suggests a uniform and probably unique source for the sulphide-sulphur. The high $\delta^{34}S_{H2S}$ values suggest the non-participation of magmatic or Early Cretaceous black-shale sulphur sources. Saline diapirs occur in the emeraldiferous areas and the most likely explanation for high $\delta^{34}S$ involves the reduction of sedimentary marine evaporitic sulphates.

Fluid-inclusion and sulphur-isotope data give a typical evaporitic sedimentary signature for Colombian emerald mineralization. This emerald-deposit type, unique in the world, corresponds to mesothermal deposits (300°C), formed in a sedimentary environment and produced through thermochemical reduction of sulphate-rich brines to hydrogen sulphide by interaction with organic-rich strata.

Key-words: Colombia, emerald, pyrite, sulphur, isotopes, fluids, evaporites.

*: present address

1. Introduction

The genesis of the hydrothermal carbonate-pyrite-emerald vein mineralization of Colombia has provoked a large debate during this century (Fallick, 1994). Firstly, the emerald mineralization was related to the circulation of magmatic-hydrothermal solutions (Scheibe, 1933; Oppenheim, 1948; Beus & Mineev, 1972). In the last 30 years, geochemical investigations (Baker, 1975; Beus, 1979; Giuliani et al., 1990a; Ottaway, 1991; Ottaway & Wicks, 1991; Cheilletz et al., 1994; Ottaway et al., 1994) converge to the model of removal of the major and trace elements from the black shales through connate waters (Medina, 1970) or basinal formation water-rock interaction (Giuliani et al., 1992). Beryllium, major and trace elements (Cr, V, REE) have a local sedimentary origin and are redistributed as infilling vein-system minerals (Giuliani et al., 1993a; Cheilletz et al., 1994; Ottaway et al., 1994).

Preliminary fluid inclusion studies on emerald crystals documented complex primary brines (Roedder, 1963, 1972, 1982; Touray & Poirot, 1968; Ottaway et al., 1986). Detailed fluid inclusion studies on emerald (Kozlowski et al., 1988; Giuliani et al., 1993b; Cheilletz et al., 1994)

showed high-salinity fluids (up to 40 wt % eq. NaCl) and the presence of other components such as calcium and potassium in the brines. The present work presents new microthermometric, SEM and Raman probe data for emerald and gangue minerals (carbonate, fluorite, quartz, parisite and pyrite) from seven emerald deposits of the eastern and western Colombian emerald zones.

Moreover, this paper presents the first sulphur isotopic data on pyrite coprecipitated with emerald and permits a discussion concerning the origin of the hydrothermal fluids.

2. Geological setting

The Colombian emerald deposits are found within two narrow zones (Fig. 1) situated along two major polyphased thrusted limits of the Eastern Cordillera corresponding to the original borders of the Cretaceous basin (Mégard, 1987). The eastern zone consists of the districts of Gachalá, Chivor and Macanal; the western zone contains the districts of Coscuez, Muzo and La Palma-Yacopí (Fig. 2). The deposits are hosted within a Early Cretaceous sedimentary series (Guavió and Macanal formations; Berriasian-
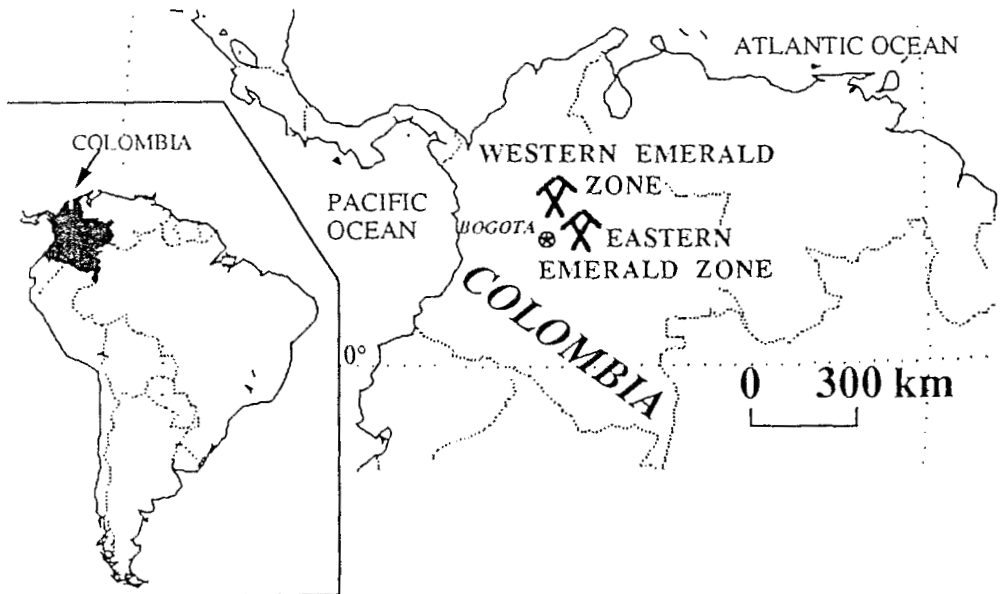

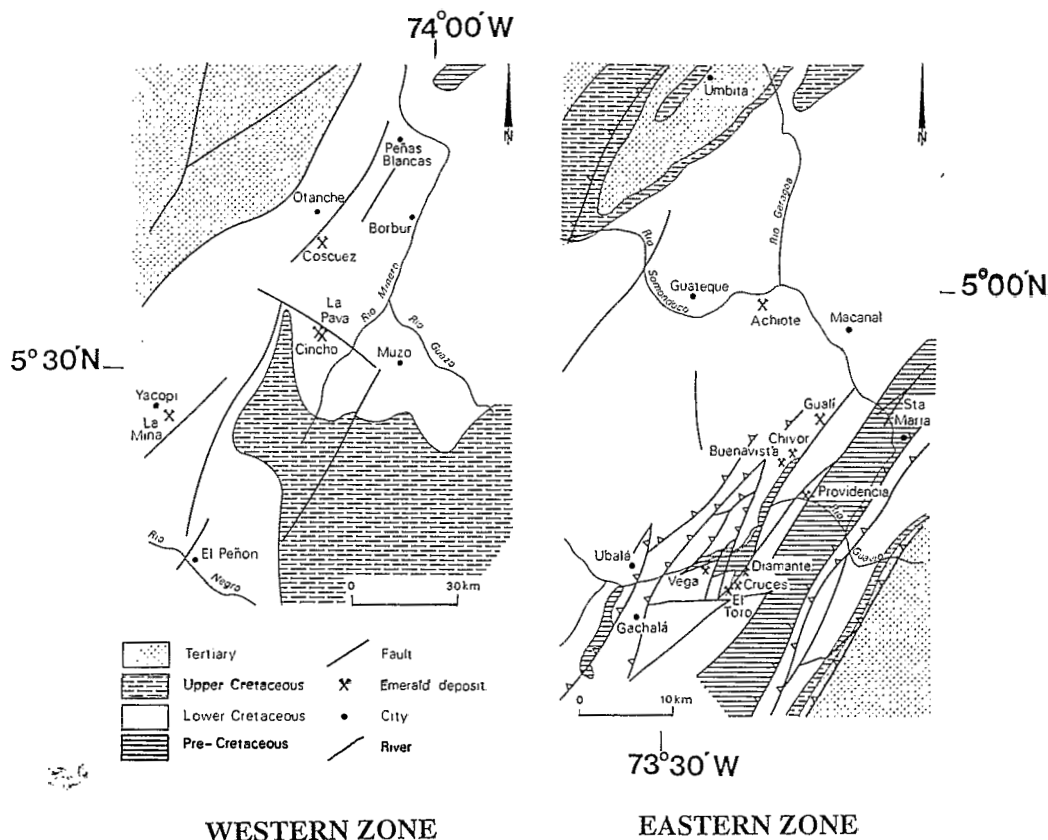Fig. 1. Location of the eastern and western Colombian emerald zones.

Fig. 2. Geological and structural environment of the eastern and western Colombian emerald zones.

Valanginian age in the eastern zone; Paja formation: Valanginian-Hauterivian age in the western zone), composed mainly of a succession of sandstones, carbonates and black shales with some horizons of sedimentary pyrite nodules. The age of emerald formation has recently been determined by $^{40}Ar/^{39}Ar$ dating on cogenetic muscovites as late Eocene-Oligocene (38-32 Ma; Cheilletz et al., 1994). The Cretaceous formations of the Eastern Cordillera are intruded by salt diapirs (Mc Laughlin & Arce, 1971) and gypsum bodies are reported in the emeraldiferous area (Ulloa & Rodriguez, 1976). However, few geological data have yet been reported on these salt occurrences.

The mineralization is hosted by breccias, networks of extension fractures and pockets related to hydrofracturing (Giuliani et al., 1990b). The hydrothermal circulation provoked an intense metasomatic alteration of the enclosing black shales which consists of albitisation, carbonatization and pyritisation halos around the mineralized structures. Emerald occurs within calcite-dolomite-pyrite veins. The mineralization sequence can be divided into three successive stages: (1) white fibrous calcite, pyrite I, albite, quartz and green micas; (2) white or grey rhombohedral calcite, dolomite, albite, pyrite II, quartz and some kerogens; (3) emerald, pyrite III, parisite, REE rich-dolomite, fluorite and quartz in drusy carbonates from stage 2.

Pyrite I is observed as euhedral cubic crystals (0.1-3 mm in size) with some octahedral moderately striated faces. Pyrite II occurs as cubic or dodecahedral crystals (0.2-2 cm). Pyrite III is found as euhedral crystals (0.2-5 cm in size) with pyritohedral and/or dodecahedral habits, observed locally as inclusions within emerald crystals.

3. Samples and analytical techniques

The microthermometric studies were performed on doubly polished plates using a microscope equipped with an UMK 50 Leitz objective and a Chaix-Meca heating-freezing stage calibrated for temperatures. The -180° to 0°C temperatures were obtained with a precision of 0.1°C; the 0° to 550°C temperatures were obtained by heating at a rate of 1°C per minute.

Raman spectra of hydrates, volatile components of the vapour phase and solid daughter minerals were obtained on a Dilor X-Y multichannel laser-excited Raman spectrometer using the 514.5 nm radiation of an Ar ion laser. The presence of volatile phases CO_2, CH_4, N_2 and H_2S was checked using a 1 W laser beam referring to the following lines, respectively: 1388 cm^{-1}, 2915 cm^{-1}, 2331 cm^{-1} and 2611 cm^{-1}.

The composition of the decrepitates, daughter crystals and solid inclusions trapped by fluid inclusions within emerald, fluorite, carbonates, parisite, quartz and pyrite was evaluated by SEM and energy-dispersive analysis. The different crystals were fractured and stuck on a support with lacquer. A conductive film of carbon was evaporated on the sample which was examined under a Cambridge Stereoscan 250 SEM, operating at an accelerating voltage of 20 kV.

The sulphur isotopic analyses were performed on sixteen hydrothermal pyrites from six emerald mines and one sedimentary pyrite (Table 1):

- Pyrite LP-3 (La Pava deposit, Muzo district) originates from a pyritic sedimentary nodule in black shale.

- Pyrites I and II were sampled in veins from unproductive emerald zones. The samples correspond to the pyrites CHI-K19, CHI-K110 (Chivor mine), YA-6A (Yacopí mine), CR-5, CR-2 (Cruces mine, Gachalá district), TOv-8c, TOm-2 (Toro mine, Gachalá district), COI-7 (Coscuez mine), and CIN-2, CIN-9 (Cincho mine, Muzo district) which present cubic and dodecahedral shapes.

- Pyrites III from productive emerald veins are the samples CHI-K112, CO-7, CIN-6, CIN-10 and YA-4A.

Pyrite bulk separates were obtained by hand-

Table 1. Sulphur isotopic data for pyrites from Colombian emerald zones.

DEPOSIT	SAMPLE	STAGE	$\delta^{34}S$	$\delta^{34}S_{H_2S}$
CHIVOR	CHI-K19	2c	15.4	14.2
	CHI-K110	2d	16.4	15.1
	CHI-K112	3d	18.1	16.9
LAS CRUCES	CR-2	2d	10.8	9.6
	CR-5	2c	10.8	9.6
EL TORO	TOm-2	1c	11.5	10.3
	TOv-8c	2c	11.4	10.2
CINCHO	CIN-2	2d	19.7	18.5
	CIN-9	2c	21.2	19.9
	CIN-6	3p	18.2	16.9
	CIN-10	3p	20.5	19.3
COSCUEZ	COI-7	2d	18.9	17.7
	CO-7	3d	20.6	19.4
YACOPI	YA-6A	2c	14.8	13.6
	YA-4A	3d,o	16.0	14.8
LA PAVA	LP-3	c	-2.4	

Eastern zone with the mining districts of Chivor, Gachalá (Las Cruces, El Toro mines) and Macanal, western zone with the mining districts of Muzo (Cincho, La Pava mines), Coscuez and Yacopí. Stages 1, 2 and 3 are indicated with the different crystal shape of pyrites: c = cubic; d: = dodecahedral; p = pyritohedral; o = octahedral. All values of $\delta^{34}S$ expressed as ‰. Values of $\delta^{34}S_{H_2S}$ are calculated with fractionation factors taken from Ohmoto & Rye (1979) assuming a temperature of mineralization at 300°C.

Table 2. Microthermometric and Raman data for fluid inclusions from emerald, quartz and dolomite from Vega San Juan, Coscuez, Chivor, Cincho, Pava and Tequendama emerald deposits.

MINE	HOST MINERAL	MICROTHERMOMETRIC DATA										RAMAN DATA	REFERENCES
		Te	TmCO2	TmC	Tmi	ThCO2	Tmhyd.	TsNaCl	TsKCl	TH (L)	TD		
VEGA SAN JUAN	Emerald	-56.1°C to -52°C	no CO2	no CO2	-35.3 to -31.6°C	no CO2	50 to 284°C	284 to 326°C (300°C)	no	215 to 330°C (235°C)	205 to 333°C (260°C)	traces CO2, carbon (DP), calcite (DP), unknown hydrate spectra	Giuliani et al. (1993b)
COSCUEZ	Emerald	-59.5 to -50.5°C	-57.9 to -56.6°C	-25.1 to -19.3°C	-33.0 to -17°C	24.3 to 30.9°C (Vapor)	4.4 to 141°C	260 to 340°C (305°C)	no	180 to 290°C (220°C)	150 to 350°C (230°C)	CO2, CO2-N2, calcite (DP), unknown hydrate spectra	Giuliani et al. (1992) Cheilletz et al. (1994)
	Quartz	no freezing data						200 to 353°C (261°C)		196 to 354°C (231°C)	172 to 342°C (244°C)		this work
CHIVOR	Emerald	no freezing data						275 to 325°C (315°C)	192°C	214 to 270°C (209°C)	194 to 323°C (255°C)		this work
CINCHO	Emerald	no freezing data						TS>TD	81°C	TH>TD	239 to 334°C (287°C)		this work
PAVA	Emerald	no freezing data						TS>TD		TH>TD	191 to 254°C (223°C)		this work
TEQUENDAMA	Dolomite	-65 to -52°C	-57.5 to -56.6°C	-26.6 to -20°C	-39 to -23°C	27.8 to 29°C (Vapor or liquid)	-3 to 27°C	TS>TH	no	TH<TS	80 to 250°C (170°C)		this work

Microthermometry: Te = eutectic temperature; Tm = temperature of final melting of: CO_2 (CO_2), C (clathrate), i (ice), hyd (hydrate); Th = temperature of homogenization of: CO_2 (liquid or vapour), or temperature of disappearance of the vapour phase (to liquid); TD = temperature of decrepitation; TsNaCl and TsKCl = temperature of final melting of halite and sylvite, respectively. *Raman data*: DP = daughter phase.

picking from concentrates; the purity of the final separates was checked by X-ray diffraction analysis. Isotopic analysis was carried out on a Finnigan-MAT Z51/45 with a dual inlet system. The sulphides were converted to SO_2 by heating at 1100°C in vacuum with excess cupric oxide in the presence of copper metal. All values of $\delta^{34}S$ are calculated using a Canyon Diablo Troilite standard. The precision of the $\delta^{34}S$ analyses is ± 0.1 permil. Results are presented in Table 1.
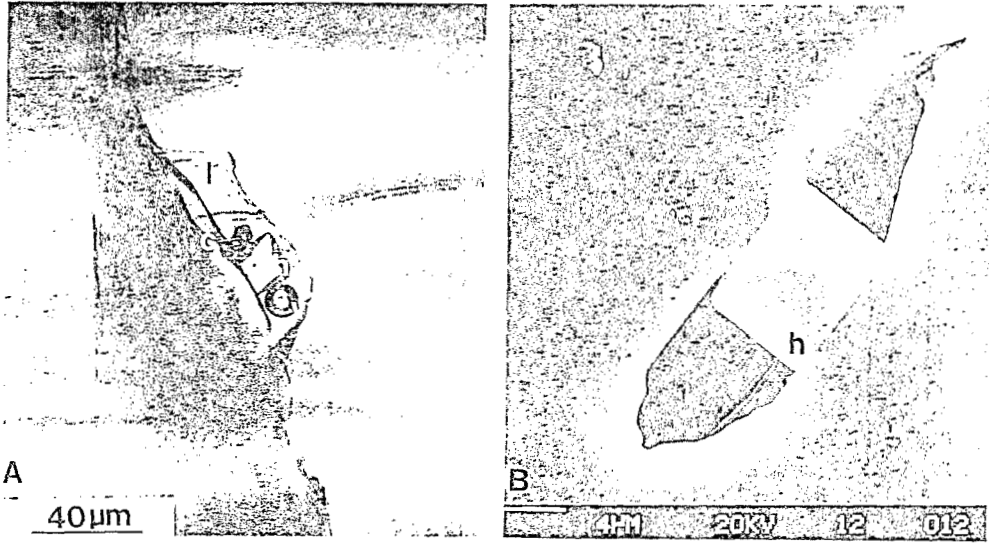
Fig. 3. Fluid inclusions hosted by emeralds. a- Transmitted light photomicrograph of pseudosecondary fluid inclusion containing halite (h) and carbonate daughter phases, a brine (l) and a vapour phase (v) (Chivor mine. Oriente workings); b- SEM microphotograph of halite (h) in a cavity of emerald fluid inclusion (Coscuez mine).

4. Fluid inclusions study

4.1. Results

Emerald

The results are presented in Table 2 together with those of former studies (Giuliani *et al.*, 1992; 1993b; Cheilletz *et al.*, 1994). These studies show the presence in all the deposits of primary three-phase (halite. brine and gas) or multiphase solid-fluid inclusions bearing $CO_{2L,v}$, N_2 in the vapour phase and daughter minerals (Fig. 3a). Halite (Fig. 3b). sylvite and other chloride components such as Ca, Fe, Mn and Cr were identified by SEM (Table 3). The presence of complex $NaCl-CaCl_2$ brines confirms the microthermometric and Raman data obtained on emerald crystals from the Coscuez and Vega San Juan deposits (Giuliani *et al.*, 1993b). During freezing experiments, eutectic temperatures ranged from -60 to -50°C and final melting temperatures of ice from -33 to -17°C, indicating the presence of Ca in the solution.

The estimation of fluid trapping temperatures in emerald inclusions is difficult mainly due to the mechanical behaviour of emerald crystals during heating (common leakage and decrepita-

tion: Kozlowski *et al.*, 1988; Cheilletz *et al.*, 1994) and the complexity of their chemical composition. Isochoric extrapolation in the $NaCl-H_2O$ system (global salinity = 37-40 wt% eq. NaCl). constrained by the $^{40}Ar/^{39}Ar$ emerald formation age and the Eastern Colombian Cordillera subsidence model, leads to a pressure-temperature estimate of 1 kbar and $300 \pm 30°C$ for the Coscuez emerald deposition (Cheilletz *et al.*, 1994).

Carbonates

We studied fluid inclusions in dolomite related to the second stage of mineral deposition from the Tequendama mine (Muzo district, western emerald zone). These 10 to 600 µm fluid inclusions are primary, pseudosecondary or secondary. Their relative phase proportions in the cavities are identical and they correspond to halite-saturated fluid inclusions (Fig. 4a, b) with halite (15 %). brine (75 %) and a gas phase (10 %). A liquid carbonic phase (LCO_2 up to 2 %) is locally visible at room temperature or observed during freezing. Another daughter mineral showing a rhombohedral habit, with high birefringence and strong anisotropy under polarized light occurs commonly in the cavities.

Table 3. SEM data for fluid inclusions and solid inclusions found in emerald, quartz, fluorite, pyrite and parisite from Vega San Juan, Coscuez, Chivor, Cincho, Tequendama, Pava and Yacopí emerald deposits.

MINE	HOST MINERAL	FLUID INCLUSIONS		SOLID INCLUSIONS
		NATURE OF THE DECREPITATES	SOLID DAUGHTER PHASES	
VEGA SAN JUAN	Emerald	NaCl; (Ca, K, Fe)Cl; KCl; (Ca, Fe)Cl	(Fe-Ti-O ?) NaCl	(Fe-O ?)
COSCUEZ	Emerald	NaCl; (K, Fe)Cl; (K, Ca, Fe)Cl; (K, Fe, Mn)Cl; (Ca, Fe)Cl; KCl; (K, Ca)Cl	NaCl; calcite; (Fe-O ?); dolomite; KCl; sphalerite	phengite quartz (Si, Al, Ca ?) dolomite
	Quartz	NaCl; KCl; (Ca, Fe)Cl	NaCl; KCl; (Fe-O ?); (Fe-Mn-O ?)	phengite
	Fluorite	NaCl; (K, Fe, Ca)Cl; KCl	KCl; NaCl	
	Pyrite	(Ca, Cl); NaCl	KCl	
CHIVOR	Emerald	NaCl; (Ca, Fe)Cl; (Ca, K, Fe, Cr)Cl	(Fe-O ?); NaCl; KCl	apatite anhydrite phengite
	Pyrite	NaCl; (Ca , Cl)	KCl	
CINCHO	Emerald	NaCl; (K, Fe, Ca)Cl; (Fe, Mn, Ca,K)Cl; (Ca, Fe)Cl; (K, Fe, Mn)Cl; KCl	NaCl; KCl	pyrite
	Pyrite	(Ca, Cl); NaCl	KCl	
	Parisite	(hematite); NaCl	NaCl	
TEQUENDAMA	Emerald	NaCl; (Ca, K)Cl; KCl	NaCl	pyrite
	Pyrite	NaCl; (Ca , Cl)	KCl	
LA PAVA	Emerald	NaCl; KCl	sphalerite	
YACOPI	Emerald	NaCl; KCl; (Ca, K, Fe)Cl; (Ca, K)Cl; (K, Fe)Cl	NaCl; KCl; dolomite parisite; Zn-carbonate; (Si, Ca, Ti, Fe ?)	pyrite

(K, Fe)Cl = salt decrepitate composed of potassium and iron; (Fe-O ?) = undetermined iron oxide.

It was identified by SEM as a Fe-Mg-rich dolomite daughter phase.

During freezing experiments (Table 2), the temperatures of final melting of CO_2 ($TmCO_2$) are in the -57.5 to -56.6°C range, indicating the presence of minor components other than CO_2 in the volatile phase. The temperatures of final melting of clathrate (Tmc) are in the -26 to -20°C
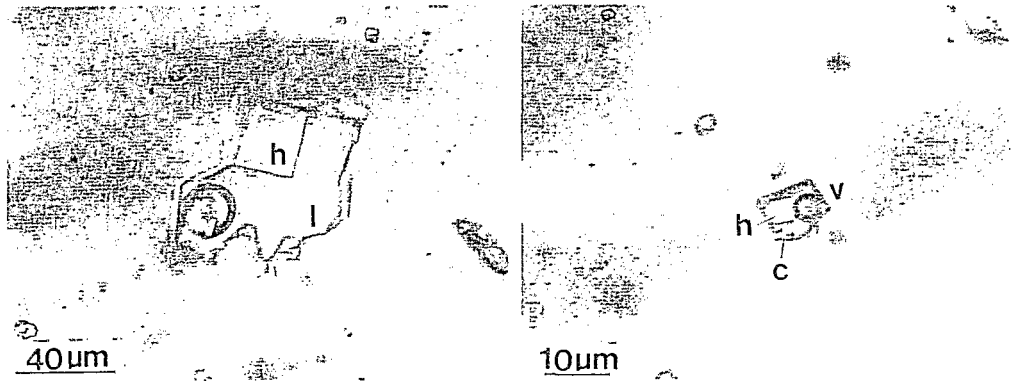
Fig. 4. Fluid inclusions hosted by carbonates. a- Transmitted light photomicrograph of typical three-phase primary fluid inclusion in dolomite showing a crystal of halite (h), a brine (l) and a vapour phase (v) (Tequendama mine, Muzo); b- Transmitted light photomicrograph of primary fluid inclusion in dolomite showing the presence of a carbonate daughter phase (c). h = halite, v = vapour (Tequendama mine, Muzo).

range. Eutectic melting temperatures, ranging from -65 to -52°C and final melting of ice from -39 to -23°C, confirm the presence of Ca^{2+} and probably other components in significant amount in the solution.

On heating, the CO_2 phase homogenizes to vapour or liquid between 27.8 and 29°C. Decrepitation and leakage affect all fluid inclusions before complete homogenization and halite melting. Decrepitation occurs at temperatures between 80 and 250°C. In some inclusions, the considerable decrease in volume of the vapour phase relative to the halite crystal before reaching the temperature of decrepitation (200 < TD < 250°C) suggests probable homogenization of the inclusions by NaCl melting.

Pyrite

Within pyrites, fluid inclusion cavities are rare and were only observed in pyrites from stages II and III through SEM analysis. Two types of fluid inclusions are recognized on the basis of their relative spatial distribution and size:

- Primary fluid inclusions are about 100 to 400 μm in size with irregular shapes. They are widespread in pyrites as isolated cavities. Generally, they contain a sylvite daughter mineral (Fig. 5a, d). The opening of the cavities during electron-beam impact led to evaporation of the infilling brines; the analysis of the decrepitates documented a mixture of Ca-Cl or Ca-Na-Cl compositions (Fig. 5c, d).

- Secondary fluid inclusions are about 10 to

50 μm in size (Fig. 5b) with irregular to negative crystal shapes and occur in trails crosscutting the primary fluid inclusions. The analysis of individual inclusion decrepitates demonstrated the presence of Na-Ca-Cl brines with significant amounts of KCl (Fig. 5b).

4.2 Discussion

The additional fluid inclusion data on Colombian emeralds and gangue minerals presented in this paper (Table 2) show that fluid inclusions homogenize by NaCl melting at temperatures between 300 and 340°C. These data fit with the temperatures of emerald formation already proposed by Ottaway *et al.* (1986), Giuliani *et al.* (1993b) and Cheilletz *et al.* (1994). They differ from the higher temperatures of complete homogenization by vapour disappearance (TH > 355°C) reported by Roedder (1982, 1984) on Chivor and Muzo mines, and Kozlowski *et al.* (1988) on the Achiote deposit (TH = 470°C). Nevertheless, the last authors explained the high temperatures obtained for emerald (up to 570°C) as the result of subtle leakage of fluid inclusions which sometimes was detected only several months after the homogenization runs. Indeed, leakage and stretching occur commonly during heating experiments for large fluid inclusions (size > 20 μm). Leakage is not always marked by a sudden reversal of the volume of the vapour phase (Vv) as temperature increases (Roedder, 1982). Sometimes, a heating run is conducted up to 550°C without significant
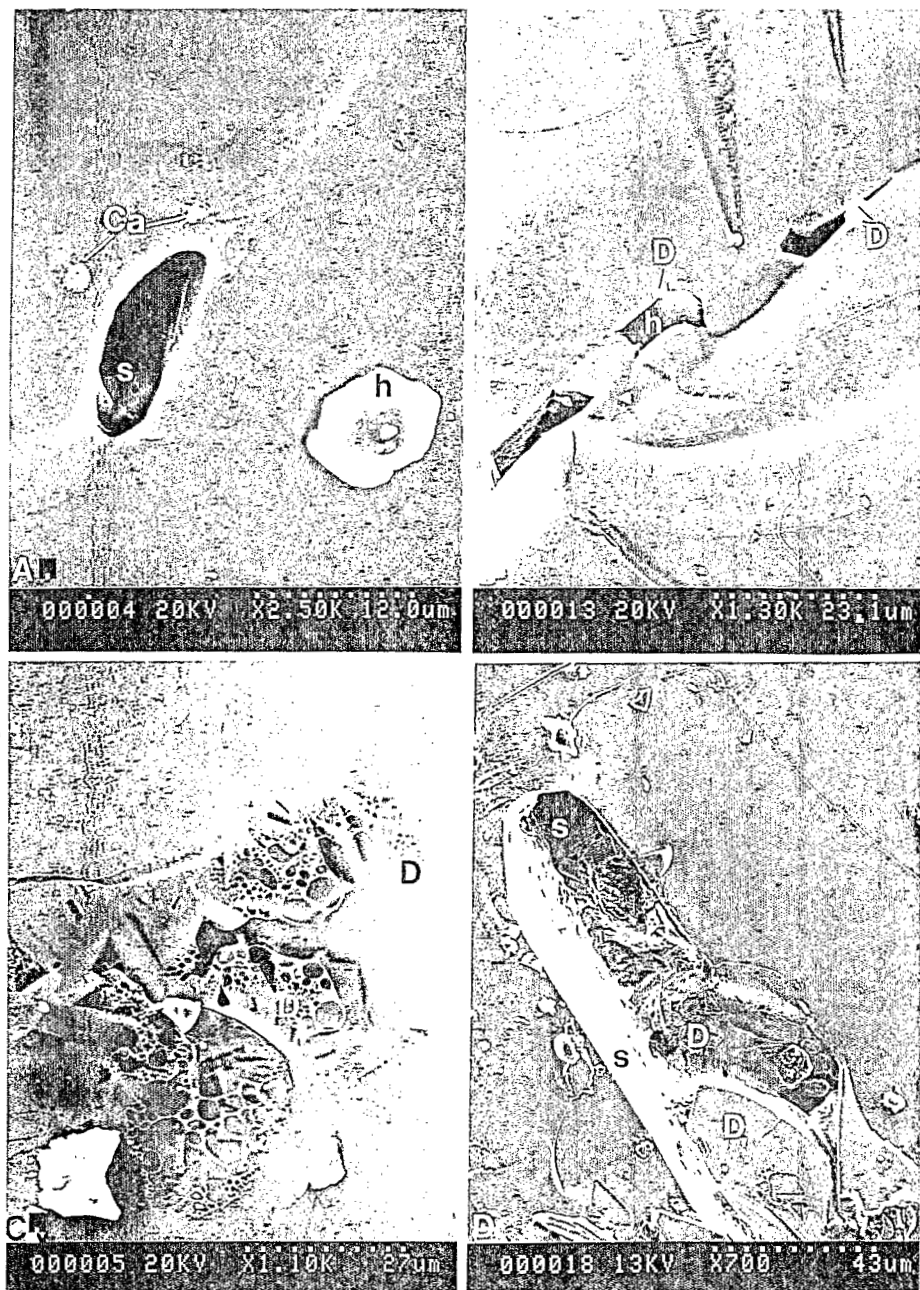
Fig. 5. Fluid inclusions hosted pyrites. a- SEM microphotograph of a fluid-inclusion-derived decrepitate salts showing a crystal of halite (h), sylvite (s) and Ca-Cl salts (Ca) (Cincho mine, pyrite III); b- SEM microphotograph showing the alignment of secondary fluid inclusions along a fracture (Cincho mine pyrite II). Note the halite daughter crystal (h) in the cavity of fluid inclusion and the presence of Na-K-Cl decrepitate salts (D); c- SEM microphotograph of Ca-Cl decrepitate (D) liberated during the electron beam impact of a sylvite daughter crystal which was sealing a fluid inclusion cavity (Chivor mine, pyrite III); d- SEM microphotograph of sylvite crystal (s) from a cavity of fluid inclusion within pyrite III (Cincho mine), covered by a film of decrepitate salts of Ca-Na-Cl composition (D).

changes. Other times, at temperatures higher than 500°C, sudden homogenization to vapour can occur. This behaviour tentatively explains the higher temperatures of homogenization obtained for emerald. The smallest inclusions (< 20 μm) contemporaneous with leaked inclusions in a single growth zone give temperatures of vapour disappearance consistent with the modal homogenization temperatures.

The temperature of deposition of carbonates associated with pyrites I and II is difficult to obtain by microthermometry because leakage and decrepitation affect all the inclusions during heating. Nevertheless, fluid-inclusion petrography and freezing experiments in carbonates show the same hypersaline brines as those found in emerald (Table 2). Inasmuch as the volume of the components of these fluid inclusions (vapour, halite, brine) is the same as in emerald, and considering that fluid inclusions homogenize in both minerals by halite disappearance, an average

temperature of 300°C is tentatively proposed for carbonates associated with pyrites I and II.

The composition of the fluids related to Colombian pyrites are K-Na-Ca-rich. Such Na-Ca brines with significant amounts of KCl are similar to the fluids associated with emerald (Giuliani et al., 1992; 1993b) and carbonate. The similarity of fluid composition in emerald, carbonate and pyrite in the eastern and western emerald zones demonstrates the homogeneity of the parent fluid and the coeval precipitation of the associated minerals.

5- Sulphur-isotope study

5.1 Results

The isotopic data for the six emerald deposits studied in this work are listed in Table 1 and reported as a function of their stratigraphic position in Fig. 6. Except for the La Pava sedimen-
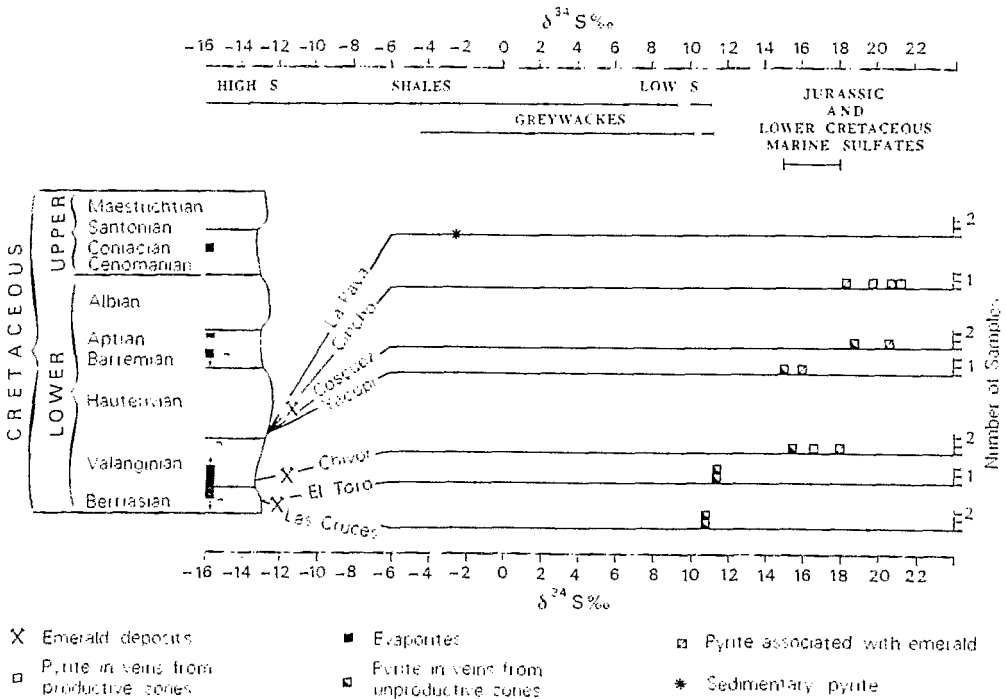

Fig. 6. Lithostratigraphic location of emerald deposits from the eastern and western Colombian emerald zones within the Early Cretaceous sedimentary series of the Eastern Colombian Cordillera. Sulphur isotopic values ($\delta^{34}S_{CDT}$) of pyrites from productive and unproductive emerald zones and $\delta^{34}S$ values of some potential sulphur sources.

tary pyrite, which yields a $\delta^{34}S$ of -2.4 ‰, the $\delta^{34}S$ of pyrites I, II and III are between 10.8 and 21.2 ‰, $i.e$ they fall in a relatively narrow range of 10 permil with a mean value of 14.9 ‰. The lowest $\delta^{34}S$ values, between 10.8 and 11.5 ‰ (samples CR-5, CR-2, TOv-8c, TOm-2), are from pyrites I and II of the emerald occurrences of El Toro and Las Cruces mines. In the Chivor, Cincho, Coscuez and Yacopí mines, the $\delta^{34}S$ values of pyrite II are lower by 2 permil than those of pyrite III.

The calculated $\delta^{34}S_{H2S}$ for the different samples are between 9.6 and 19.9 ‰ (Table 1). They were obtained assuming equilibrium fractionation of sulphur, using the isotopic fractionation factors (Ohmoto & Rye, 1979) and the average temperature of deposition (300°C) deduced from the fluid inclusion study.

5.2 Interpretation

The narrow spread in $\delta^{34}S_{H2S}$ from pyrite III ($14.8 < \delta^{34}S_{H2S} < 19.4$ ‰), cogenetic with emerald deposition in the Colombian deposits, suggests (1) that the sulphur isotopic composition of the ore-forming fluids is uniform and, (2) the sulphide-sulphur source is heavy and probably unique. Moreover, the results of the fluid inclusion study show the presence of homogeneous and hypersaline brines which belong to the H_2O-$NaCl$-KCl-$CaCl_2$-CO_2-N_2 system. These two distinct and complementary geochemical approaches converge towards a model involving $NaCl$-KCl-$CaCl_2$-rich brines originated from sedimentary evaporitic sulphate as the source of the sulphide-sulphur component of the mineralizing fluids.

In fact, salt diapirs are known to intrude the Late Cretaceous series in the Sabana of Bogotá (Zipaquirá and Nemocon mines), and the Early Cretaceous series in the eastern emerald zone (Mc Laughlin, 1972). Lopez $et\ al.$ (1988) proposed a minimum Valanginian age for the sedimentary deposition of the evaporitic layers, and Campbell & Burgl (1965), based on favourable conditions for evaporite deposition during the breaking of Pangea, proposed a Jurassic age for the deposition of salt in Colombia. This episode of evaporite formation during the North Atlantic opening can be traced from the Triassic-Jurassic in North America and Peru, up to the Aptian-Albian in Brazil, Venezuela and western Africa (Lopez $et\ al.$, 1988). However, horizons of sedi-

mentary evaporites have not, to this date, been found in the Jurassic or the Early Cretaceous formations of the Eastern Cordillera of Colombia. Considering that gypsum diapirs are found in the vicinity of emerald deposits in the eastern emerald zone, this makes the existence of salt levels below the Early Cretaceous series highly probable. These salt levels might have been percolated by deep basinal formation waters (Giuliani $et\ al.$, 1992) during the ore-forming hydrothermal process. Therefore, the most likely explanation for the sulphur isotopic data involves the reduction of sedimentary Early Cretaceous and/or Jurassic marine sulphates. In fact, worldwide marine sulphates display mean values of $\delta^{34}S$ as high as 15 to 18 permil for this period (Holser & Kaplan, 1966; Claypool $et\ al.$, 1980; Dejonghe $et\ al.$, 1989, see Fig. 6); this $\delta^{34}S$ range overlaps the $\delta^{34}S_{H2S}$ of pyrites associated with Colombian emeralds.

The comparison of calculated $\delta^{34}S_{H2S}$ values for pyrite III with inferred $\delta^{34}S$ values for evaporitic sulphate is not strictly valid. However, it is known that the sulphur isotopic composition ($\delta^{34}S_{\Sigma S}$) of the different sulphur-bearing species in the hydrothermal solution, which reflects the source of sulphur, must be at least as heavy as the maximum value of calculated $\delta^{34}S_{H2S}$ for sulphide (Ohmoto, 1972). Therefore, the only likely and unique source of sulphur as heavy as 19.4 ‰ might be sulphur derived from evaporites through a sulphate reduction process at the site of mineral precipitation.

5.3 Discussion

Two main objections to this interpretation of sulphur isotope data can be addressed. High $\delta^{34}S$ values can result, (1) from an originally heavy source submitted to an oxygen fugacity decrease with time during the precipitation of pyrite and emerald, and (2) from the gradual addition of sulphur from an isotopically heavy source to an originally light source, either magmatic ($\delta^{34}S = 0 \pm 3$ ‰) or sedimentary.

Objection (1) is not valid. In fact, the precipitation of the mineral assemblage occurred within the stability field of pyrite at an fO_2 value buffered by the enclosing black shales.

Objection (2) can also be rejected: the participation of a light magmatic source is highly improbable considering the lack of any igneous activity during the emerald formation process

(Cheilletz *et al.*, 1994). The participation of sedimentary sulphur can be viewed through the $\delta^{34}S$ data on sedimentary pyrites from the Early Cretaceous series. One $\delta^{34}S$ value of -2.4 ‰ has been measured on the La Pava sedimentary pyrite (Fig. 6). This unique $\delta^{34}S$ value is evidently not sufficient to characterize the whole sedimentary sulphide reservoir formed by the Early Cretaceous black shales. However, this value falls within the typical range of $\delta^{34}S$ values (mean = -12 ± 5 ‰) expected for diagenetic pyrite in black shales (Holser & Kaplan, 1966; Wedepohl, 1978). Moreover, a contribution for sulphide-sulphur composition from the host-rock black shale adjacent to the mineralized veins would have scattered the $\delta^{34}S$ values as result of a mixing process. The consistency and the uniformity of the $\delta^{34}S$ data found for the Colombian pyrites eliminates such a possible mechanism.

The fractionation of sulphur isotopes is also well known as acting during the thermochemical reduction of sulphate by organic matter. Although this mechanism was probably working during the vein formation and pyrite deposition, the absolute variation induced is thought to be less than 10 ‰ for the $\delta^{34}S$ values (Macqueen & Powell, 1983). This range is comprised within the measured variation range of Colombian pyrites and thus cannot be distinguished.

There are three other major features that can be deduced from the data presented in Fig. 6:

- The overall variation of $\delta^{34}S$ within stratigraphic height from the eastern and western Colombian emerald zones (11.4 < $\delta^{34}S$ < 18.1 ‰ for the Berriasian and 14.8 < $\delta^{34}S$ < 21.2 ‰ for the Hauterivian host-rocks, respectively; Fig. 6) is a prominent feature which merits a discussion. A likely explanation, as suggested by Seal (1994, pers. comm.), is that as sulphate-rich brines traverse the organic-rich strata of the Early Cretaceous series, thermochemical reduction of the brine sulphate to H_2S by interaction with organic matter and precipitation of pyrite causes the residual sulphate to become progressively enriched in $\delta^{34}S$, which is then reduced and precipitated higher in the stratigraphic sequence. However, this interpretation cannot be applied to the studied emerald occurrences, considering that within a single deposit, no important $\delta^{34}S$ variation is observed. Moreover, the tectonic style of the Eastern Cordillera, albeit poorly known, precludes the existence of complete stratigraphic series in the vicinity of the emerald deposits, because of the presence of thrusting and decolle-

ment structures. In such tectonics, salt horizons of Jurassic age (for instance) might directly underlie the Berriasian or Hauterivian strata. The enrichment in $\delta^{34}S$ through interaction with organic matter during the percolation of hydrothermal fluids might then be effective for a single propagating vein during its vertical extension.

- The $\delta^{34}S$ values of pyrite II are lower than those of pyrite III (Fig. 6). Three possible explanations can be advanced: (1) precipitation of pyrite can increase the $\delta^{34}S$ of the residual H_2S; (2) decreasing temperature from stages II to III can produce a similar effect. The average temperature of deposition for pyrite (300°C) was estimated from microthermometric data obtained on coeval carbonates. Fluid-inclusion data are not comprehensive enough to exclude a variation of temperature from stage II to III, which can be roughly estimated to be at most -100°C, considering the nature of the mineral assemblage in the veins (Cheilletz *et al.*, 1994). Such a variation would produce a 1 ‰ variation in $\delta^{34}S$ values, which could explain the observed variation between pyrite II and III; (3) a third explanation for this variation is the probable change in the SO_4^{2-}/H_2S ratio of the fluid, assuming that sulphide precipitating from solutions contain both H_2S and SO_4^{2-} species. The decreasing of the mSO_4^{2-}/mH_2S could be correlated to a decrease of fO_2 during pyrite III deposition. A more reduced state (lower SO_4^{2-}/H_2S ratio) is enhanced by the closing of the vein system as a consequence of fluid-pressure variations and crystallization of vein-filling minerals. The third explanation appears to be the most likely.

- Pyrites I and II (El Toro and Las Cruces mines, Fig. 6), display low $\delta^{34}S$ values in the range 10.8 to 11.5 ‰ (Table 1). These lightest $\delta^{34}S$ values can be explained considering two major points: (1) fluctuations of the oxidation state and/or the pH of the solution during deposition would produce such light values (Ohmoto & Rye, 1979), assuming that redox equilibrium existed in the solution at 300°C; (2) sulphate reduction by reaction with organic matter (Ohmoto & Lasaga, 1982; Macqueen & Powell, 1983) as proposed by Ottaway *et al.* (1994) for the Muzo deposit. For these authors, according to the model of Powell & Macqueen (1984) for the Pine point MVT Pb-Zn deposit, reactions of sulphate-rich brines and pyrobituminen-derived H_2S in carbon-rich black shales reduced thermochemically the sulphate to H_2S. Following the iterations of the reaction between hydrogen sulphide

formed by cracking of organic matter (low $\delta^{34}S$ values) and coeval sulphide (high $\delta^{34}S$ values), the reactant sulphur would present intermediate $\delta^{34}S$ values, lower than those of the parent sulphate.

6- Conclusions

Fluid-inclusion and sulphur-isotope data strongly support a hydrothermal sedimentary model for the Colombian emerald mineralization. The fluid-inclusion study has revealed Na-Ca-K-bearing hypersaline chlorine brines. The $\delta^{34}S$ values of pyrites from the Colombian emerald veins are isotopically heavy. The most likely interpretation involves the reduction of sedimentary derived marine sulphates of evaporitic origin.

Other geochemical data permit better constraints to be placed on the model (Giuliani et al., 1992; Cheilletz et al., 1994): (1) carbon isotopes obtained from carbonates show the participation of limestone and organic matter for the origin of carbon ($\delta^{13}C$), (2) calculated $\delta^{18}O$ of H_2O for quartz and carbonates in equilibrium with the mineralization have a basinal formation waters signature, (3) the major-element chemistry of emerald-forming fluids indicates the same Na-Ca-K-Cl composition observed in oil-field brines and MVT mineralizing fluids (Hall & Friedman, 1963; White, 1974; Sverjensky, 1981; Roedder, 1984) which are similar also to basinal brines (Carpenter et al., 1974; Haynes & Kesler, 1987), fluids associated to Pb-Zn deposits related to salt diapirs (Guilhaumou et al., 1981) or metamorphosed evaporites (Mc Kibben et al., 1988).

This sedimentary contribution is also demonstrated by the behaviour of trace elements (Be-Cr-V) constituting the vein-filling minerals (Giuliani et al., 1990a, 1993a) which clearly are derived from the leaching of enclosing black shales. However, the temperature and pressure conditions (300 ± 30°C, 1 kbar) of emerald precipitation (Cheilletz et al., 1994) are higher than those found in basinal formation waters (Sheppard, 1984) or recorded in Mississippi Valley Type sulphide deposits (T < 210°C; Roedder, 1984). Comparison between thermobarometric data for emerald deposition and burial temperature estimates of the Eastern Cordillera basin (Hébrard, 1985; Fabre, 1987) requires an additional 120 to 150°C thermal input with regard to the burial temperatures of the enclosing black shales. Cheilletz et al. (1994) considered two possible heat sources: (1) synchronous magmatism and (2) heat conduction implemented during halokinetic ascent. Magmatic intrusions do not occur in the emeraldiferous area and hypothesis (1) can thus be excluded. Hypothesis (2) is more likely, considering that the geothermal gradient in salt dome environments varies as a function of the geographic location and depth. At the transition between hydropressurized and geopressurized zones, the geothermal gradient increases considerably, as for instance in the Gulf Coast Salt domes, where the gradient reaches 50 to 75°C per kilometre in the vicinity of salt domes (Jones, 1975). Considering the close relationship existing between emerald deposits and evaporitic horizons, the sulphate-rich brines responsible for emerald and pyrite deposition correspond to deep-seated formation waters, heated by burial, thereafter dissolving evaporites by interaction with salt diapirs.

The most significant conclusions are that Colombian emerald deposits are unique in the world and differ drastically from the well-known biotite-schist-emerald deposit-type (Sinkankas & Read, 1986; Schwarz, 1987; Giuliani et al., 1990c; Kazmi & Snee, 1990) which are related to granite-pegmatite environments. The Colombian deposits correspond to mesothermal deposits (300°C), formed in a sedimentary environment and produced through thermochemical reduction of sulphate-rich brines to hydrogen sulphide by interaction with organic-rich strata.

References

Baker, P. J. (1975): Projecto de esmeraldas. Informe tecnico final Naciones Unidas-Ingeominas, COL-72/004, 71 p.

Beus, A. A. (1979): Sodium: a geochemical indicator of emerald mineralization in the Cordillera Oriental. Colombia. *J. Geochem. Explor.*, II, 195-208.

Beus. A. A. & Mineev, D. A. (1972): Some geological and geochemical features of the Muzo-Coscuez emerald zone. Cordillera Oriental, Colombia. Informe Ingeominas, Bogotá, unpubl. rep., 50 p.

Campbell, C. J. & Burgl. H. (1965): Section through the Eastern cordillera of Colombia, South America. *Geol. Soc. America Bull.*, 76, 567-590.

Carpenter, A. B., Trout, M. L., Pickett, E. E. (1974): Preliminary report on the origin and chemical evolution of lead and zinc-rich oil field brines in central Mississippi. *Econ. Geol.*, 69, 1191-1206.

Cheilletz, A., Féraud, G., Giuliani, G., Rodriguez, C. T. (1994): Time-pressure and temperature constraints on the formation of Colombian emeralds: $^{40}Ar/^{39}Ar$ laser microprobe and fluid inclusion study. *Econ. Geol.*, 89, 361-380.

Claypool, G. E., Holser, W. T., Kaplan, I. R., Sakai, H., Zak, I. (1980): The age curves of sulfur and oxygen isotopes in marine sulfate and their mutual interpretation. *Chemical Geol.*, 28, 199-260.

Dejonghe, L., Boulègue, J., Demaiffe, D., Létolle, R. (1989): Isotope geochemistry (S, C, O, Sr, Pb) of the Chaudfontaine mineralization (Belgium). *Mineralium Deposita*, 24, 2, 132-140.

Fabre, A. (1987): Tectonique et génération d'hydrocarbures: un modèle de l'évolution de la Cordillère Orientale de Colombie et du bassin des Llanos pendant le Crétacé et le Tertiaire. *Arch. Sc. Genève*, 40, 2, 145-190.

Fallick, A.E. (1994): The new treasure seekers. *Nature*, 369, 522-523.

Giuliani, G., Cheilletz, A., Rodriguez, C. T. (1990a): New metallogenic data on the emerald deposits of Colombia. 8th IAGOD Symposium, Ottawa, 12-18 August 1990, Abstracts, 185-186.

Giuliani, G., Rodriguez, C. T., Rueda, F. (1990b): Les gisements d'émeraude de la Cordillère orientale de la Colombie: nouvelles données métallogéniques. *Mineralium Deposita*, 25, 105-111.

Giuliani, G., Silva, L. J. H. D., Couto, P. (1990c): Origin of emerald deposits of Brazil. *Mineralium Deposita*, 25, 57-64.

Giuliani, G., Sheppard, S. M. F., Cheilletz, A. (1992): Fluid inclusions and $^{18}O/^{16}O$, $^{13}C/^{12}C$ isotope geochemistry contribution to the genesis of emerald deposits from the Oriental Cordillera of Colombia. *C. R. Acad. Sci. Paris*, 314, Série II, 269-274.

Giuliani G., Cheilletz, A., Sheppard, S. M. F., Arboleda, C. (1993a): Geochemistry and origin of the emerald deposits of Colombia. 2nd Biennal SGA Meeting, Granada 9-11 september 1993. Extended Abstracts, 105-108.

Giuliani, G., Cheilletz, A., Dubessy, J., Rodriguez, C. T. (1993b): Chemical composition of fluid inclusions in Colombian emerald deposits. Proceedings of the Eight Quadriennal IAGOD Symposium, 159-168.

Guilhaumou, N., Dhamelincourt, P., Touray, J. C., Touret, J. (1981): Etude des inclusions fluides du système N_2 CO_2 de dolomites et de quartz de Tunisie septentrionale. Données de la microcryoscopie et de l'analyse à la microsonde à effet Raman. *Geochim. Cosmochim. Acta*, 45, 657-673.

Hall, W. E. & Friedman, I. (1963): Composition of fluid inclusions, Cave-In-Rock fluorite district, Illinois, and upper Mississippi Valley zinc-lead district. *Econ. Geol.*, 58, 886-911.

Haynes, F. M. & Kesler S. E. (1987): Chemical evolution of brines during Mississippi Valley-Type mineralization: evidence from East Tenessee and Pine Point. *Econ. Geol.*, 82, 53-71.

Hébrard, F. (1985): Les foot-hills de la Cordillère Orientale de la Colombie entre les rios Casanare et Cusiana. Evolution géodynamique depuis l'Eo-Crétacé. Unpublished doctoral thesis. Paris, Université Pierre et Marie Curie, 162 p.

Holser, W. T. & Kaplan, I. R. (1966): Isotope geochemistry of sedimentary sulfates. *Chemical Geol.*, 1, 93-135.

Jones, P.H. (1975): Geothermal and hydrocarbon regimes, northern Gulf of Mexico Basin, in Proceedings of the First Geothermal Energy Conference, Extension Publications, University of Texas, Austin. 15-90.

Kazmi, A. H. & Snee, L. W. (1990): Emeralds of Pakistan. Geology, gemmology and genesis. A.H. Kazmi and L.W. Snee, ed., Geol. Survey Pakistan-Van Nostrand Reinhold Co., 269 p.

Kozlowski, A., Metz, P., Jaramillo, H. A. E. (1988): Emeralds from Somondoco. Colombia: chemical composition, fluid inclusions and origin. *N. Jb. Mineral. Abh.*, 159, 23-49.

Lopez, C., Briceno, A., Buitrago, J. (1988): Edad y origen de los diapiros de sal de la Sabana de Bogotá. III Simposio bolivariano "Exploracion petrolera en las cuencas subandinas", Agosto 1988, Bogotá, 28 p.

Macqueen, R. W. & Powell, T. G. (1983): Organic geochemistry of the Pine Point lead-zinc ore field and region, Northwest Territories, Canada. *Econ. Geol.*, 78, 1-25.

Mc Kibben, M. A., Williams, A. E., Okuko, S. (1988): Metamorphosed Plio-Pleistocene evaporites and the origins of hypersaline brines in the Salton Sea geothermal system, California: Fluid inclusions evidence. *Geochim. Cosmochim. Acta*, 52, 1047-1056.

Mc Laughlin, D. & Arce, M. (1971): Recursos minerales de parte de los departamentos de Cundinamarca, Boyacá y Meta. *Bol. Geol. Ingeomin.*, **19**, 1, 1-102.

Mc Laughlin, D. H. (1972): Evaporite deposits of Bogotá area, Cordillera oriental, Colombia. *American Association of petroleum Geologists*, **56**, 2240-2259.

Medina, L. F. (1970): Consideraciones sobre la genesis de los yacimientos esmeraldiferos de Muzo. II Congresso Colombiano de minas, Manizalès, Ecominas ed., 10-20.

Mégard, F. (1987): Cordilleran Andes and Marginal Andes: A review of Andean geology North of Arica Elbow (18 deg. S). *in* "Circum Pacific ocean", Monger, J. W. H. & Francheteau, J., eds. *Am. Geophys. Union, Geodynamics Series*, **18**, 71-95.

Ohmoto, H. (1972): Systematics of sulfur and carbon isotopes in hydrothermal ore deposits. *Econ. Geol.*, **67**, 551-578.

Ohmoto, H. & Lasaga, A. C. (1982): Kinetics of reactions between aqueous sulfates and sulfides in hydrothermal systems. *Geochim. Cosmochim. Acta*, **46**, 1727-1745.

Ohmoto, H. & Rye, R. O. (1979): Isotopes of sulfur and carbon. *in* "Geochemistry of hydrothermal ore deposits", Barnes H. L. , ed. Wiley New York, 509-567.

Oppenheim, V. (1948): The Muzo emerald zone, Colombia S.A. *Econ. Geol.*, **43**, 31-38.

Ottaway, T. L. (1991): The geochemistry of the Muzo emerald deposit, Colombia. Master Thesis, University of Toronto.

Ottaway, T. L. & Wicks, F. J. (1991): Sulfate reduction at the Muzo emerald deposit, Colombia. GAC-MAC Joint Annual Meeting with Society of Economic Geologists, Toronto, 27-29 May 1991, Abstracts, p. 93.

Ottaway, T. L., Wicks, F. J., Bryndzia L.T., Spooner, E.T.C. (1986): Characteristics and origin of the Muzo emerald deposit, Colombia. IMA Meeting, Abstracts with programs, Stanford, California, p. 193.

Ottaway, T. L., Wicks, F. J., Bryndzia L.T., Kyser, T.K., Spooner, E.T.C. (1994): Formation of the Muzo hydrothermal emerald deposit in Colombia. *Nature*, **369**, 552-554.

Powell, T.G. & Macqueen, R.W. (1984): Precipitation of sulfide ores and organic matter: sulfate reactions at Pine Point, Canada. *Science*, **224**, 63-66.

Roedder, E. (1963): Studies of fluid inclusions II: freezing data and their interpretation. *Econ. Geol.*, **58**, 163-211.

— (1972): Composition of fluid inclusions. *US. Geol. Surv. Prof. Paper*, **440** JJ, 1-164.

— (1982): Fluid inclusions in gemstones: valuable defects. Proceedings Int. Gemol. Symp., Santa Monica, **1**, 479-502.

— (1984): Fluid inclusions. *Rev. Mineral., Mineralog. Soc. Amer.*, **12**, 644 p.

Scheibe, R. (1933): Informe geológico sobre la mina de esmeraldas de Muzo. *Boletim de Minas*, 20-32.

Sheppard, S.M.F. (1984): Stable isotope studies of formation waters and associated Pb-Zn hydrothermal ore deposits. *in* "Thermal phenomena in sedimentary basins", D. Durand, ed. Technip, Paris, 301-317.

Schwarz, D. (1987): Esmeraldas-inclusões em gemas. Imprensa Universitaria UFOP Ouro Preto, Brazil, 450 p.

Sinkankas, J. & Read, P. (1986): Beryl. Butterworths Gem Books, 225 p.

Sverjensky, D. (1981): The origin of a Mississippi Valley-type deposit in the Viburnum trend, southeast Missouri. *Econ. Geol.*, **76**, 1848-1872.

Touray, J. & Poirot, J. P. (1968): Observations sur les inclusions fluides primaires de l'émeraude et leurs relations avec les inclusions solides. *C. R. Acad. Sci. Paris*, sér. D., **266**, 305-308.

Ulloa, M. C. & Rodriguez, M. E. (1976): Geologia del cuadrangulo K-12, Guateque. Informe 1701 Ingeominas, *Bol. Geol.*, **22**, 1, 1-55.

Wedepohl, K.H. (1978): Handbook of Geochemistry 16B, ed. Berlin Heidelberg New York, Springer, 1-40.

White, D. E. (1974): Diverse origins of hydrothermal ore fluids. *Econ. Geol.*, **69**, 954-973.